

Supplementary Information

Kozina et al, "Terahertz-Driven Phonon Upconversion in SrTiO₃"

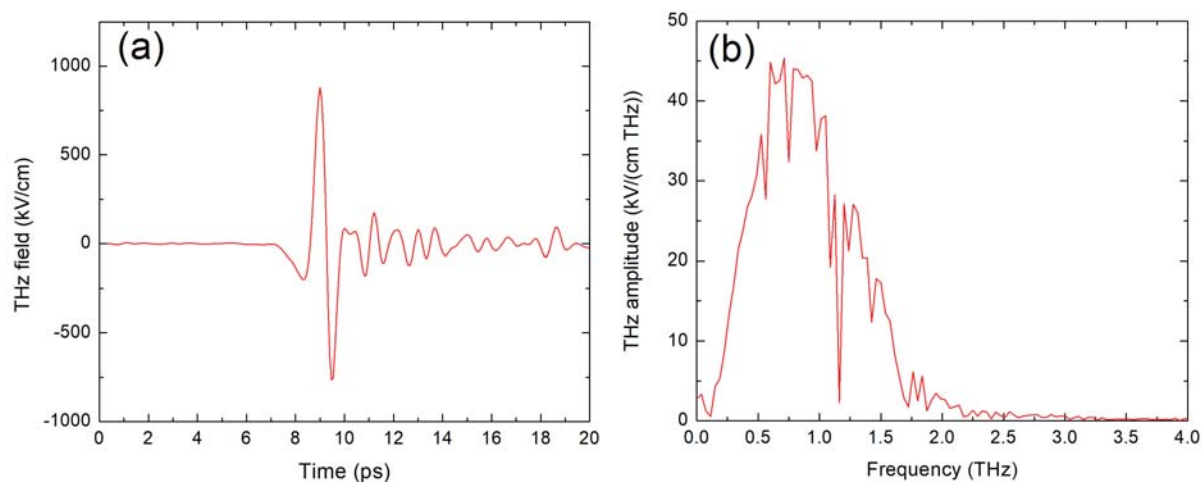


Figure S1 Terahertz pump waveform: **a** Electro-optic sampling signal of terahertz (THz) pump at sample location measured in-situ by electro-optic sampling in a 50 μm thick (110) GaP crystal. **b** Magnitude of frequency spectrum of the THz waveform in **a** calculated by Fast Fourier Transform. The intensity was adjusted with wiregrid polarizers (Infraspecs P01) without changing the THz waveform.

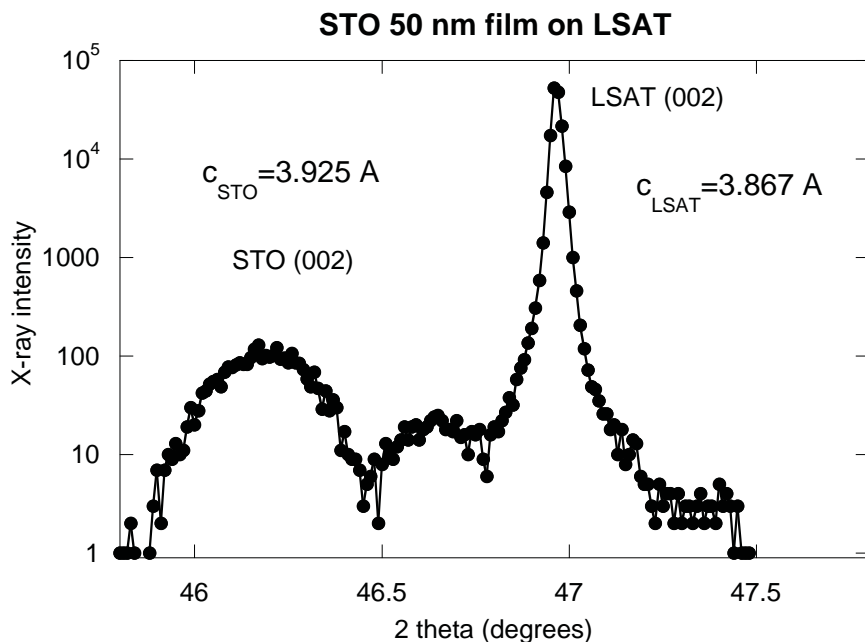


Figure S2: Two-Theta scan of sample before annealing. Static x-ray diffraction pattern along sample normal. The low-angle peak corresponds to the STO film and the sharp peak at higher angle is the LSAT substrate. We observe clear splitting along the cross-plane direction between the substrate and the film. These measurements were taken before the sample was annealed.

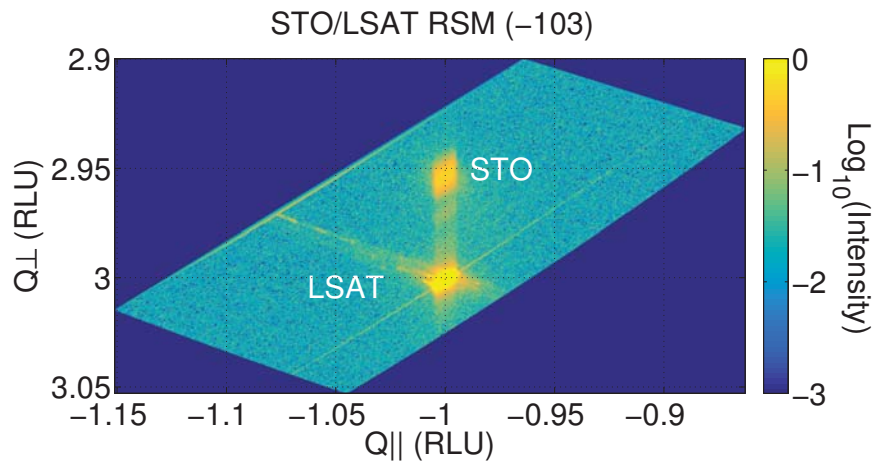


Figure S3: Reciprocal space map of the sample before annealing. Static reciprocal space map collected on a similar sample prior to annealing about the $(-1\ 0\ 3)$ reciprocal lattice point using a $\text{Cu } \alpha$ source. The separation between the film and substrate peaks along the cross-plane direction shows there is a difference in lattice parameter, whereas there is clear indication that in-plane the film and substrate are lattice matched to the LSAT unit cell.

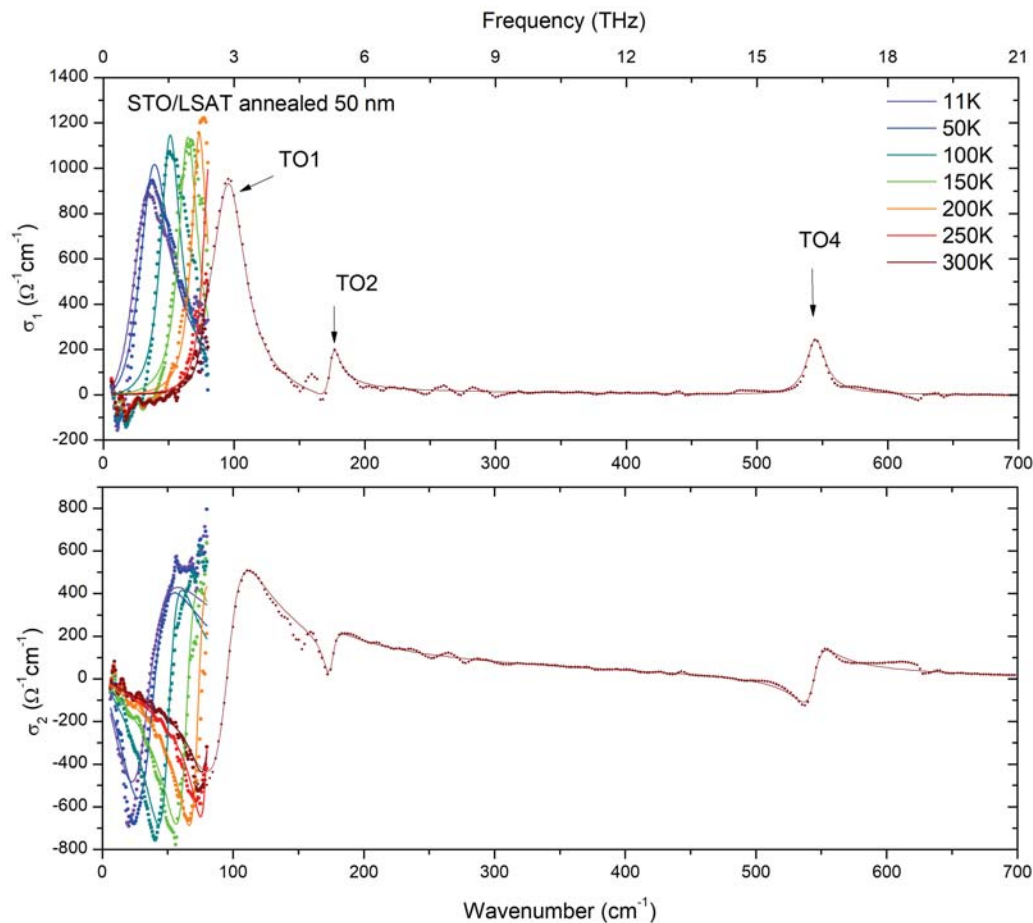


Figure S4: Optical conductivity of the annealed sample. We show additional ellipsometry measurements on our sample incorporating extra temperature points at low and high temperature. The extended frequency range at 300K shows the TO_2 and TO_4 phonon modes. Data from Fig. 3a are also included for comparison.

	Sr	Ti	Oxy	Ozx	Oyz
X	0	0.5	0.5	0.5	0
Y	0	0.5	0.5	0	0.5
Z	0.00987045	0.51190984	0.9970011	0.4956093	0.4956093

Table S1 Unit Cell Relative Coordinates from DFT. Lattice is tetragonal with $a_0 = 3.89000 \text{ \AA}$ and $c_0 = 3.91043 \text{ \AA}$.

	Sr	Ti	Oxy	Ozx	Oyz
X	0.02963898	0.04544241	-0.08189972	-0.09030182	-0.07348941
Y	-0.02957567	-0.04530107	0.08204853	0.07359076	0.09041028
Z	0	0	0	0	0

Table S2 Eigenvector for Q_1 mode. Eigenvector calculated with E_{THz} parallel to $(X, -Y, 0)$. The units of the eigenvector are $\text{\AA}^* \text{AMU}^{1/2}$. The eigenvector is normalized so that $\sum \xi_{ijk}^2 m_{jk} = 1$. Here ξ_{ijk} and m_{jk} are the eigenvector and ion mass in AMU, and the indices i, j, k label the eigenvector mode, ion, and coordinate direction.

	Sr	Ti	Oxy	Ozx	Oyz
X	-0.04831474	0.07770832	0.01575631	0.00874036	0.00874793
Y	0.04829799	-0.07773579	-0.01568512	-0.00870886	-0.00868356
Z	0	0	0	0	0

Table S3 Eigenvector for Q_2 mode. Eigenvector calculated with E_{THz} parallel to $(X, -Y, 0)$. The units of the eigenvector are $\text{\AA}^* \text{AMU}^{1/2}$. The eigenvector is normalized so that $\sum \xi_{ijk}^2 m_{jk} = 1$. Here ξ_{ijk} and m_{jk} are the eigenvector and ion mass in AMU, and the indices i, j, k label the eigenvector mode, ion, and coordinate direction.

$\omega_1/(2\pi)$	1.669 THz	κ_1	$8900 \text{ THz}^2 \text{\AA}^{-2} \text{AMU}^{-1}$	χ	$4000 \text{ THz}^2 \text{\AA}^{-2} \text{AMU}^{-1}$
$\omega_2/(2\pi)$	5.186 THz	κ_2	$1066 \text{ THz}^2 \text{\AA}^{-2} \text{AMU}^{-1}$	ψ_{12}	$-4000 \text{ THz}^2 \text{\AA}^{-2} \text{AMU}^{-1}$
$\gamma_1/(2\pi)$	0.900 THz	Z_1^*	$2.6 \text{ e}^- \text{AMU}^{-1/2}$	ψ_{21}	$-841 \text{ THz}^2 \text{\AA}^{-2} \text{AMU}^{-1}$
$\gamma_2/(2\pi)$	0.150 THz	Z_2^*	$0.2 \text{ e}^- \text{AMU}^{-1/2}$	β	0.215

Table S4 Model parameters. Values in bold are unmodified from DFT calculations at 0 K. Values in red were extracted from spectroscopy and literature. Parameters κ_1 , ψ_{12} , and χ were initially established by DFT and then tuned to best fit the experimental data. The parameter β was informed by calculations for the expected field screening inside the STO film on the LSAT substrate but was fine-tuned to best fit the experimental data. The linewidth γ_2 was estimated from the trXRD data in the frequency domain.

Comments on Mode Symmetry in STO Film

In bulk STO, there are four sets of optical phonons, with symmetries (in order of increasing frequency) T_{1u} , T_{1u} , T_{2u} , and T_{1u} [S1]. The three T_{1u} modes are all IR active and in addition possess LO/TO splitting. The T_{2u} mode is known as “silent” because it lacks both IR and Raman activity [S2]. This mode lacks TO/LO splitting. The mode frequencies at 85K are presented in Table S5 and labeled according to [S3].

Mode	Frequency (cm ⁻¹)	Frequency (THz)
TO ₁ (soft)	31	0.93
LO ₁	170.6	5.114
TO ₂	172.5	5.171
T _{2u} (TO ₃ , LO ₂) (silent)	265	7.94
LO ₃	469.5	14.08
TO ₄	544	16.3
LO ₄	801	24.0

Table S5 Bulk STO Mode Frequencies at 85 K. Values are extracted from Barker [S3].

In our film, however, the substrate is compressive and makes the STO film slightly tetragonal (see static x-ray characterization in Figure S2). This changes the space group to $P4mm$ and the point group at zone center to $4mm$ (C_{4v}). Therefore this alters the symmetries of the four modes according to the rules: $T_{1u} \rightarrow A_1 + E$, $T_{2u} \rightarrow B_1 + E$. The A_1 and B_1 modes consist of displacements along the cross-plane component, while the E modes consist of displacements in-plane. This splitting should also adjust the frequencies of the modes.

The incident THz field resonantly couples to a near-zone center transverse optical mode (the soft mode) with displacement along the THz polarization direction, $[1 -1 0]$, and with wavevector parallel to the THz wavevector (cross-plane direction). Thus the excited soft mode has displacement vector along $[1,-1,0]$ and wavevector along $[0 0 1]$, and has symmetry E . In addition to observing this feature in our trXRD signal, we also detect oscillations at 5.15 THz and 7.6 THz, close in frequency to the LO₁/TO₂ and T_{2u} (silent) modes in bulk STO.

By symmetry, we can only couple the E -symmetry soft mode to other modes of symmetry E by a fourth-order coupling term (e.g. $Q_1^2 Q_2^2$ or $Q_1^3 Q_2$). Additionally, our x-ray scattering geometry is only sensitive to motion with some component parallel to the x-ray scattering vector, along $[2 -2 3]$. In-plane, this corresponds to the $[1 -1 0]$ direction.

Thus, while we can couple to E modes with polarization along $[1 1 0]$ we cannot detect them with our choice of x-ray scattering geometry. Our x-ray scattering geometry is also sensitive to displacements in the cross-plane direction $[0 0 1]$ however these modes are symmetry A_1 and therefore require a different coupling term. Specifically, at lowest order we would have either $Q_1^2 Q_2$ and then $Q_1^4 Q_2$. These features would manifest respectively as signal at $2 * \omega_1/2\pi$ (3.3 THz) and $4 * \omega_1/2\pi$ (6.7 THz) which we do not observe.

Hence we attribute the oscillatory components at 5.15 and 7.6 THz in our x-ray scattering signal to transverse optical phonons with symmetry E with displacements along $[1 -1 0]$

and wavevectors along $[0\ 0\ 1]$. We then label these three coupled modes as TO_1 , TO_2 , and TO_3 in order of increasing frequency. Note that from our numerical calculations of the nonlinear phonon coupling terms, we find that $T_{1u}(\text{soft}) \rightarrow T_{2u}(\text{silent})$ coupling while possible is much weaker than $E(\text{soft}) \rightarrow E(\text{silent})$.

References:

S1. Cowley, R. A. Lattice Dynamics and Phase Transitions of Strontium Titanate. *Phys. Rev.* **134**, A981–A997 (1964).

S2. Denisov, V. N., Mavrin, B. N., Podobedov, V. B. & Scott, J. F. Hyper-Raman Spectra and Frequency Dependence of Soft Mode Damping in SrTiO₃. *J. Raman Spectrosc.* **14**, 276–283 (1983).

S3. Barker, A. S. Temperature dependence of the transverse and longitudinal optic mode frequencies and charges in SrTiO₃ and BaTiO₃. *Phys. Rev.* **145**, 391–399 (1966).